Unwrapping of Nucleosomal DNA Ends: A Multiscale Molecular Dynamics Study

Karine Voltz,[†‡] Joanna Trylska,[§] Nicolas Calimet,[¶] Jeremy C. Smith,[‡||] and Joerg Langowski[†]

[†]Biophysics of Macromolecules, German Cancer Research Center, Heidelberg, Germany; [‡]Computational Molecular Biophysics, Interdisciplinary Center for Scientific Computing, University of Heidelberg, Heidelberg, Germany; [§]Interdisciplinary Centre for Mathematical and Computational Modeling, University of Warsaw, Warsaw, Poland; [¶]Computational Biochemistry, Interdisciplinary Center for Scientific Computing, University of Heidelberg, Heidelberg, Germany; and [||]Center for Molecular Biophysics, Oak Ridge National Laboratory, Oak Ridge, Tennessee

Supporting Material

Methods

Preparation of the model structure

The nucleosome simulated contains the eight histones with their tails and 167 bp of DNA: the 147 bp corresponding to the NCP DNA with two 10-bp DNA linkers added at each end. We prepared this structure by superimposing the NCP structure (PDBid 1KX5) (1) on one nucleosome of the tetranucleosome structure (PDBid 1ZBB) (2). Since 1ZBB was solved by molecular replacement using 1KX5, the RMSD between the structures of the common protein part is almost zero (0.05 Å) while the RMSD for the common 147-bp DNA part is 1.43 Å, the last turn of DNA on each side of the nucleosome showing the highest RMSDs. The DNA superhelix of 1KX5 was then substituted with 167-bp DNA of 1ZBB (147 bp of core DNA and 20 bp of DNA linkers). This hybrid assembly was finally energy minimized in solution as described in "All-atom molecular dynamics" in "Methods". An H3-tailless structure was also prepared by removing residues 1 to 42 of the histones H3 of the model structure.

Coarse-grained model: adjustments for the nucleosome with DNA linkers

Force constants were derived for P–P interactions in the DNA linkers and for P–P pairs in the SH6.5 and SH-6.5 DNA segments. Test simulations showed that the description of pseudobonded and bp P–P interactions of the DNA linkers with the parameters formerly calculated for the nucleosomal DNA leads to the loss of their helical structure. Likewise, the SH-6.5 DNA segment was unstable when detached from the histone core (see "Results"). This was expected since the helical parameters were derived only for nucleosomal DNA that is bent and bound to a protein core. The new force constants (in Suppl. Mat.) were obtained by applying the same procedure as used previously (3) to a 5-ns all-atom MD simulation of a 15-bp DNA segment in explicit solvent. The force constants for P-P pairs in DNA linkers are $\approx$ 1.5-3 times higher than those obtained for nucleosomal DNA, which is consistent with maintaining the DNA double helix. The Morse parameters for nonbonded interactions in the linkers and in the SH-6.5 and SH6.5 segments were kept the same as for the nucleosomal DNA and the equilibrium distances for pairs involving residues in these regions were taken from the minimized starting model of the nucleosome. The force constants calculated for P-P pairs in the DNA linkers were also assigned to P-P pairs of the SH-6.5 and SH6.5 segments and the equilibrium distances of pairs involving residues from these later segments were taken from the minimized starting model of the nucleosome.

Table 1: Aditionnal CG parameters used for describing P–P contacts in the DNA linkers and the SH-6.5 and SH6.5 DNA segments. Force constants k_{1-1+n} are given in kcal/mol/Å^2, interbead equilibrium distances r^0_{1-1+n} and cutoff in Å, and α in Å^{-1}. The functional forms are described in (3).

Harmonic potentials	
k_{1-2}	5
k_{1-3}	1.5
k_{1-4}	1
k_{pb}	0.6
r^0_{1-2}	6.8
r^0_{1-3}	13
r^0_{1-4}	18
r^0_{pb}	19.3
Morse potentials	
α	0.707
$D_{\mathrm{e}}(r^0_{i,i+n})$	$exp(-r^0_{i,i+n}/6.0)$
r_0 for long-range inter.	26.3
$cutoff$	24

All-atom molecular dynamics

The all-atom MD system of the closed-state nucleosome was set up and energy minimized using the program CHARMM (4) and the CHARMM27 force field (5). MD was performed with the program NAMD (6). The all-atom system was prepared as described above (see "Model structure") and then was solvated with a buffer of explicit water extending at least 15 Å from the surface of the nucleosome in each direction in a tetragonal box (x=156 × y=156 × z=84 Å). The system was neutralized by adding 158 Na^+ counterions while providing an excess of 110 Na^+ and Cl^- ions corresponding to a physiological concentration of 150 mM NaCl. The addition of the ions was carried out by random substitution of water oxygens. The solvated structure with ions (≈198,000 atoms; 87% solvent) was minimized using 5000 steps of steepest descent then with the conjugate gradient algorithm until a tolerance gradient of 0.004 kcal/mol/Å was satisfied.

The temperature of the system was gradually increased during a 300-ps MD heating phase from 0 to 300 K with random reassignment of velocities every 1 ps. The system was then

equilibrated in two different phases: in the first 120 ps atomic velocities were rescaled every 1 ps. In the second 4.8-ns phase, the temperature was maintained using Langevin dynamics with a damping coefficient of 2 ps^{-1} applied to each atom. Pressure control was introduced in this second phase using a Nosé-Hoover Langevin piston (7, 8) with a period of 100 fs and decay time of 50 fs. All bonds containing hydrogen were frozen with the SHAKE algorithm (9), enabling an integration timestep of 2 fs to be used.

The 100-ns production simulation was performed in the NPT ensemble at a 1-atm. pressure and 300 K using periodic boundary conditions. Electrostatic interactions were treated with the Particle Mesh Ewald method (10) on a 156 × 156 × 84 charge grid, with sixth-order B-spline interpolation. Van der Waals interactions were truncated at 12 Å using a switch function (11) starting at 10 Å.

A similar scheme was used for the MD simulation of the all-atom model reconstructed from the P and C_α positions of the CG structure representative of the long-lived open state (see "Methods"). To account for the detached DNA end, a larger box of solvent (x=168 × y=168 × z=96 Å) and hence a wider PME charge grid (160 × 160 × 96) were used. An excess of 120 Na^+ and Cl^- ions (150 mM NaCl) were added after charge neutralization. In order to help stabilizing the DNA segment that is detached from the histone core, the ions were distributed iteratively according to the electrostatic potential recalculated after adding every single ion starting from the desolvated nucleosome. After energy minimization and heating to 300 K as described above, the system (≈264,000 atoms; 90% solvent) was subjected to 15 ns of equilibration in three steps of 5 ns each: P and C_α positions restrained by a 1 kcal/mol/A^2 force constant and all base pairs maintained with distance restraints (see "Methods"); gradual release of the positional restraints; and gradual release of the distance restraints between base pairs. The final 100 ns production was performed without any restraints in the NPT ensemble as described above for the closed-state nucleosome.

MM-PBSA calculations

In order to assess that the long-lived open state of the nucleosome is not an artefact of the CG force-field, conformation-dependent free energy calculations were performed using the all-atom models. Following the MM-PBSA approach (12–15) the absolute conformational free energy of the solute molecule in state i is derived from averaging over MD trajectory snapshots:

$$G^i = \langle E^i_{MM} \rangle + \langle G^i_{PB} \rangle + \langle G^i_{SA} \rangle - TS^i_{MM} \quad (1)$$

where $\langle E^i_{MM} \rangle$ is the average gas-phase molecular mechanics energy, $\langle G^i_{PB} \rangle$ and $\langle G^i_{SA} \rangle$ are the averages of, respectively, electrostatic (Poisson–Boltzmann) and non-polar (surface area-dependent) contributions to the solvation free energy, and TS^i_{MM} is the vibrational entropy at the simulation temperature. Here, absolute free energies of both closed and long-lived open states of the nucleosome were estimated from their respective 100 ns all-atom MD trajectories.

The enthalpic contributions to the absolute free energy of the solute alone extracted from each all-atom trajectory snapshot were calculated as follows using the CHARMM program. The gas-phase E^i_{MM} term was recomputed with the CHARMM27 force-field for bonded and non-bonded terms, using an infinite cutoff and no PME. The electrostatic free energy of solvation G^i_{PB} of the highly-charged nucleosome was computed by solving the full (non-linearized) Poisson–Boltzmann equation over a 3D grid with the Adaptive Poisson–Boltzmann Solver (16) through the iAPBS interface. The nucleosome interior and solvent medium were assigned a dielectric constant of 1 and 80, respectively. A 1.4 Å radius probe sphere together with atomic radii optimized for amino acids (17) and nucleotides (18) allowed to delineate the dielectric boundary that was further smoothed using a 0.4 Å cubic spline window. The CHARMM27 atomic partial charges

and dielectric constant values were mapped over the grid using a cubic B-spline discretization method. A 150 mM salt concentration was set with Boltzmann-distributed charges and radii corresponding to NaCl solution at 300 K. The numerical solver used an automatically-configured sequential focusing multigrid calculation, with an initial grid extending 20 Å away from the solute atoms, a 0.5 Å grid spacing and single Debye-Hückel boundary conditions. Smaller grid spacings did not significantly influence the final average solvation energy. The non-polar solvation term G^i_{SA} was estimated by computing the total solvent-accessible surface area (SASA) using a 1.4 Å radius probe sphere and the CHARMM27 atomic radii, such as:

$$\left\langle G^i_{SA} \right\rangle = \gamma \times SASA + \beta \tag{2}$$

where γ=0.00542 kcal/(mol.A^2) and β=0.92 kcal/mol are, respectively, surface tension and correction terms (19) suitable for G^i_{PB} calculated at room temperature.

The vibrational entropy term TS^i_{MM} of state i of the desolvated nucleosome was estimated from quasi-harmonic analysis (20) over the corresponding 100 ns MD trajectory. All solvent and hydrogen atoms were discarded from the trajectories, and the overall rotational and translational motion of the solute heavy atoms was removed by superimposing all snapshots on the average structure using mass weighting. The cartesian covariance matrix resulting from the atom-positional fluctuation tensors was mass-weighted and diagonalized to obtain the quasi-harmonic modes from which the vibrational entropy was derived at 300 K using the VIBRAN module of CHARMM. Higher-order correction terms (21, 22) were not applied due to the system size.

Results

Movie of a short- and long-lived detachments

The movie depicts a short and a long-lived detachments occuring on 328 ns in simulation 1.

Contacts involved in the short-lived detachment

The native contacts that are broken and the new contacts formed during the short-lived DNA detachments were identified by monitoring the distances between residues of the SH-6.5 DNA end and the neighboring histones, and the distances between residues of H3 tail and residues in its vicinity (see "Methods") and are shown in Fig.1

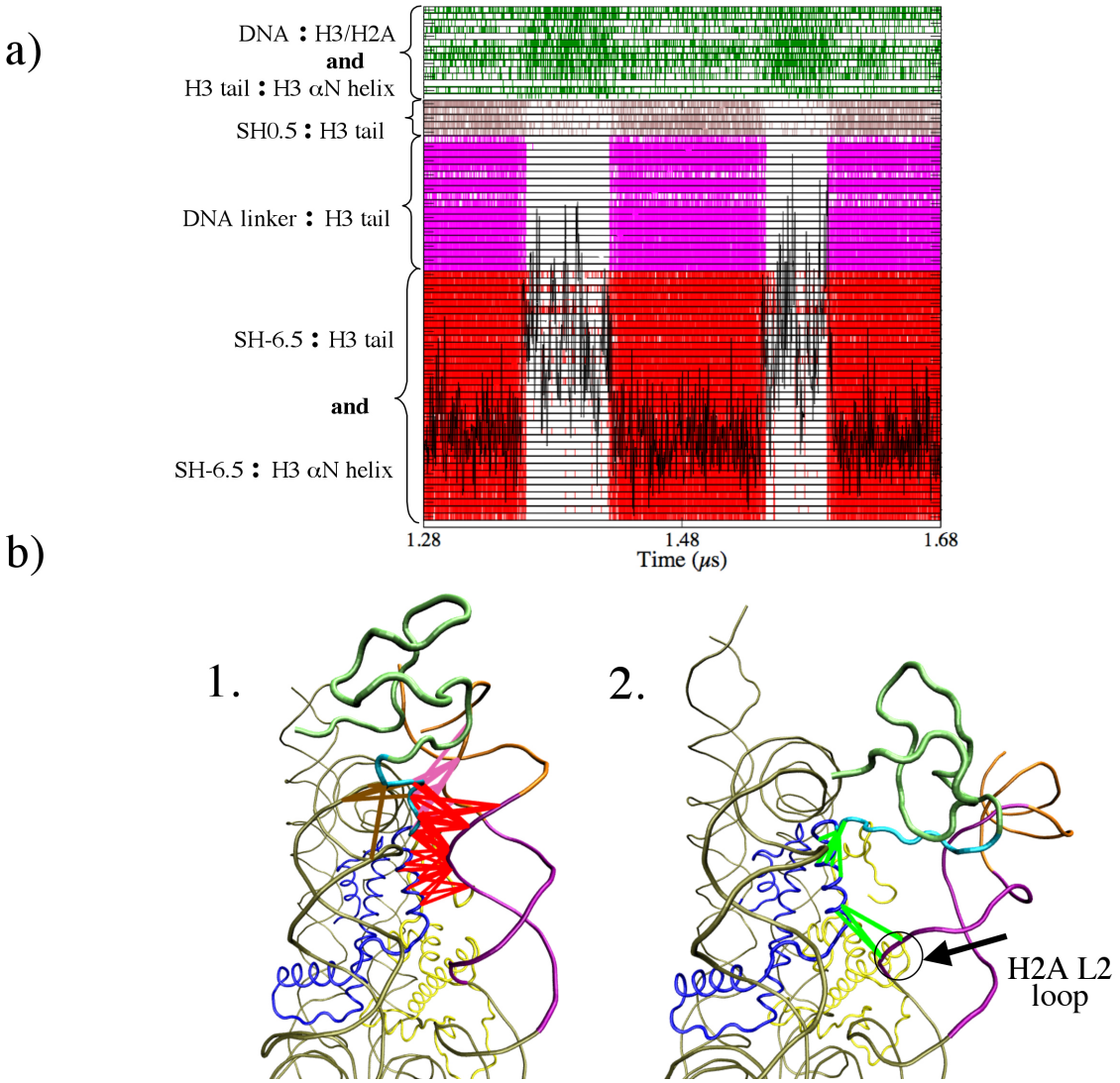

Figure 1: (a) Formed and broken contacts during two SH-6.5 end detachments occurring between 1.28 μs and 1.68 μs in simulation 1. A green tick is displayed if a non-native contact is formed. The absence of red, magenta or brown ticks means that a native interaction is broken (see "Methods"). (b 1.) Representation of the nucleosome in a closed state with the native contacts that are broken during the detachment (red, magenta and brown lines): nine residues of the H3 αN helix (residues 42, 45, 46, 48-51, 53 and 56) and seven residues of the base of the H3 tail (residues 35 to 41) participate in these broken contacts. Contacts are also broken between the DNA linker and the base of the H3 tail. Contacts also break between residues 35 to 41 of the tail and residues from the SH0.5 DNA segment (b 2.). Representation of the nucleosome in an open state with the contacts that are formed (green lines): contacts are formed between residues 40 and 41 of the tail and residues 44-49 of the H3 αN helix. Basepairs of the SH-6.5 DNA end come closer to residues 53 and 55 of the H3 αN helix and to residues 69, 72 and 74 of loop L2 of H2A.

Details of the hydrogen bonds in the all-atom mapped structure

Table 2: Hydrogen bonds present in the region of the turn-like structure calculated from the 24 ns simulation of the all-atom MD of the mapped structure (distance between the hydrogen and the acceptor <2.4Å).

base of the H3 tail : SH-6.5 DNA end	
pairs	occupancy
LYS36 N - O1P ADE14	35.0%
LYS36 NZ - O2P ADE14	38.4%
LYS36 NZ - O1P ADE14 LYS36 NZ - O2P ADE15 LYS36 NZ - O2P THY16	23.0%
base of the H3 tail : SH0.5 DNA segment	
TYR41 N - O1P ADE91	75.5%
ARG40 NH2 - N3 ADE90 ARG40 NH2 - O1P CYT92	17.3%

Details of the hydrogen bonds in the model structure

Table 3: Hydrogen bonds between the histone H3 α-N helix and the SH-6.5 DNA segment calculated for the 10-ns simulation of the nucleosome model, i.e. in the closed configuration (distance between the hydrogen and the acceptor <2.4Å).

base of the H3 tail : SH-6.5 DNA end	
pairs	occupancy
ARG42 N - O1P CYT154	99.3%
ARG42 NH2 - O2P ADE155	81.3%
THR45 OG1 - O1P CYT154	97.6%
ARG53 NH1 - O2P ADE15	34.4%
LYS56 NZ - O1P THY16	96.1%

Free energy difference of the closed and long-lived open states

Absolute conformational free energies of the closed and long-lived open states were estimated from their respective 100 ns all-atom MD trajectories. The enthalpic contributions were calculated for 200 snapshots for each state; however, 19 early snapshots in the closed-state trajectory resulted in unrealistic G_{PB} energies and these insufficiently relaxed conformations were discarded. The estimates of the vibrational entropies were obtained from all of the quasi-harmonic modes (42,789) of the solute heavy atoms obtained over the full-length trajectories (100,000 frames each).

Table 4 summarizes the calculated enthalpic and entropic contributions to the conformational free energies and the predicted free energy difference. All three G_{MM}, G_{PB}, and G_{SA} terms show a stabilization of the closed state by 564.6 kcal/mol over the long-lived open state. Conversely, the latter gains vibrational entropy in almost the same margin ($-T\Delta S_{MM} = 491.7$ kcal/mol) at 300 K. Overall, these estimates predict that the long-lived open-state of the nucleosome sits in a free energy basin about 73 kcal/mol higher than that of the closed-state. Within the framework of the MM-PBSA approach, such a free energy difference is reasonable given the system size and limited accuracy of the method as discussed below.

The largest contribution to the enthalpic term arises from the electrostatic solvation free energy; this is expected given the large, highly charged system. However, on average, G_{PB} contributes the least to the free energy difference between the closed and long-lived open states as a result of compensating effects. On the one hand, the detachement of the DNA in the long-lived open state exposes charges to the solvent that were screened by opposite charges when packed over the histones in the closed state. On the other hand, the H3 tail charges, while solvent-screened in the closed state, come into close interaction with the opposite charges of the acidic patch in the long-lived open state, resulting in their effective screening. Another significant contribution comes from the molecular mechanics G_{MM} term. Consistent with he loss of interaction energy within the nucleosome when the SH-6.5 DNA segment detaches away, the non-bonded (electrostatic and dispersion) contributions are significantly larger in the open state. The detachment occurs without inducing any unrealistic structural distortion since the internal (bonded) term marginally differs between the two states. Finally, the non-polar G_{SA} term contributes the least to the free energy differencel; as expected, the exposed surface area is larger in the long-lived open state.

Note that the free energy differences for G_{PB} and G_{MM} (electrostatic term mostly) are much smaller than the corresponding, overlapping energy fluctuations in each state. Therefore, while consistent with a destabilization of the long-lived open state, the enthalpic contribution to the free energy difference may be overestimated in particular if the respective states of the nucleosome were insufficiently relaxed over the 100 ns simulations (i.e. too short a sampling for such a large system in explicit solvent).

By contrast to the enthalpic destabilization, the vibrational entropy favors the long-lived open state, yet to a lesser extend. Preliminary results of per-residue entropy estimates in each state (data not shown) indicate that the larger entropy in the open state arises in part from the detached DNA fragment which gains enhanced mobility. However, while intuitively consistent with a more flexible open state, the accuracy of the entropic estimates is limited and the corresponding free energy difference is most likely overestimated. For instance, using half the number of MD snapshots (50,000) in the entropy calculations lead to a conformational free energy difference ≈20% larger in favor of the closed-state. Similarly, the quasi-harmonic approach is questionable (23) in particular when applied to the long-lived open state for which the detached DNA segment may undergo slow global motions crossing multiple free energy basins. We believe that much longer all-atom simulations are needed to overcome the phase-space sampling

problems in the quasi-harmonic formalism and which would also require the computation of correction terms (22). Alternatively, one may proceed instead by performing normal mode analysis on multiple MD snapshots, requiring extensive and careful energy minimizations. Such an accurate entropy calculation goes beyond the scope of the present study and shall be addressed using e.g. microsecond-timescale, higher-temperature and/or umbrella sampling all-atom MD simulations of the nucleosome closed and open states.

The MM-PBSA approach is an approximate method that is not routinely applied for obtaining conformational free energies, especially in the case of molecular systems involving nucleic acids (15). However, this is the only existing method that can be used to study large and complex systems such as the nucleosome within a reasonable amount of time. One must bear in mind that the method has numerous limitations and approximations (13). For example, the G_{PB} term depends on the solution of the Poisson-Boltzmann equation which is a mean-field theory, depends on the force field parameters (such as atomic radii) as well as on the definition of the dielectric boundary. The non-polar SASA term is also parameter dependent; however, the contribution coming from the change of G_{SA} is not large in comparison with the other terms (Table 4) so we believe the parameter set of equation 2 can be taken as a standard one for use with the CHARMM27 force-field. Even though some of the terms have reasonable absolute values and signs (such as TS_{MM} which is larger in the more flexible open-state), one can only discuss and analyze our results in terms of relative energetics and not absolute ones.

In summary, the calculations of the conformational free energies show consistent results between the closed and a long-lived open state of the nucleosome. The conformational free energy difference, while overestimated, remains within acceptable bounds for such a complex system. One may view the long-lived open state as an intermediate configuration of the nucleosome sitting in a free energy basin slightly above that of the closed state. In such an intermediate state, the nucleosome would be waiting to relax in another lower-energy state where e.g. the DNA would detach from the histone core further away, possibly involving a longer DNA segment. Such processes would occur on timescales that are not attainable by the present all-atom as well as coarse-grained simulations. As it stands, one may conclude that both states are very likely to co-exist in well-balanced populations.

Table 4: Absolute and relative conformational free energies (kcal/mol) calculated with the MM-PBSA formalism.

	Closed state	Long-lived open state	$\Delta G_{closed-open}$
	Average enthalpic contributions[a]		
G_{MM}[b]	43701.7 (988.8)	44240.6 (979.9)	-538.9
electrostatic	9883.4 (923.3)	10128.6 (931.3)	-245.2
dispersion	-5495.4 (93.8)	-5214.2 (87.9)	-281.2
internal	39313.7 (130.2)	39326.2 (124.0)	-12.5
G_{PB}	-116017.2 (1363.9)	-116009.9 (989.5)	-7.3
G_{SA}	477.2 (9.9)	495.6 (5.8)	-18.4
total	-71838.3 (972.6)	-71273.7 (804.0)	-564.6
	Entropic contributions[c]		
TS_{MM}	20690.5	21182.2	-491.7
	Conformational free energy		
G	-92528.8	-92455.9	-72.9

[a]values averaged over 181 (closed state) or 200 (open state) all-atom MD snapshots, standard deviation in parenthesis.

[b]decomposed into electrostatic, dispersion (van der Waals) and internal (bonded) contributions.

[c]estimated by quasi-harmonic analysis over 100,000 all-atom MD snapshots.

References

1. Davey, C. A., D. F. Sargent, K. Luger, A. W. Maeder, and T. J. Richmond, 2002. Solvent mediated interactions in the structure of the nucleosome core particle at 1.9Å. *J. Mol. Biol.* 319:1097–1113.

2. Schalch, T., S. Duda, D. Sargent, and T. Richmond, 2005. X-ray structure of a tetranucleosome and its implications for the chromatin fibre. *Nature* 436:138–141.

3. Voltz, K., J. Trylska, V. Tozzini, V. Kurkal-Siebert, J. Langowski, and J. Smith, 2008. Coarse-grained force field for the nucleosome from self-consistent multiscaling. *Journal of Computational Chemistry* 29:1429.

4. Brooks, B., R. Bruccoleri, B. Olafson, D. States, S. Swaminathan, and M. Karplus, 1983. CHARMM: A program for macromolecular energy, minimization, and dynamics calculations. *J. Comput. Chem.* 4:187–217.

5. MacKerell, J. A., N. Banavali, and N. Foloppe, 2001. Development and current status of the CHARMM force field for nucleic acids. *Biopolymers* 56:257–265.

6. Phillips, J. C., R. Braun, W. Wang, J. Gumbart, E. Tajkhorshid, E. Villa, C. Chipot, R. D. Skeel, L. Kale, and K. Schulten, 2005. Scalable molecular dynamics with NAMD. *J. Comput. Chem.* 26:1781–1802.

7. Martyna, G. J., D. J. Tobias, and M. L. Klein, 1994. Constant pressure molecular dynamics algorithms. *The Journal of Chemical Physics* 101:4177–4189.

8. Feller, S. E., Y. Zhang, R. W. Pastor, and B. R. Brooks, 1995. Constant pressure molecular dynamics simulation: The Langevin piston method. *The Journal of Chemical Physics* 103:4613–4621.

9. Ryckaert, J. P., G. Ciccoti, and H. J. C. Berendsen, 1977. Numerical integration of the Cartesian equations of motion of a system with constraints: Molecular dynamics of $n-$alkanes. *J. Chem. Phys.* 23:327–341.

10. Darden, T., L. Perera, L. Li, and L. Pedersen, 1999. New tricks for modelers from the crystallography toolkit: the particle mesh Ewald algorithm and its use in nucleic acid simulations. *Structure* 7:R55–R60.

11. Steinbach, P. J., and B. R. Brooks, 1994. New Spherical-Cutoff Methods for Long-Range Forces in Macromolecular Simulation. *J. Comput. Chem.* 15:667–683.

12. Srinivasan, J., T. E. Cheatham, P. Cieplak, P. A. Kollman, and D. A. Case, 1998. Continuum Solvent Studies of the Stability of DNA, RNA, and Phosphoramidate–DNA Helices. *Journal of the American Chemical Society* 120:9401–9409.

13. Kollman, P. A., I. Massova, C. Reyes, B. Kuhn, S. Huo, L. Chong, M. Lee, T. Lee, Y. Duan, W. Wang, O. Donini, P. Cieplak, J. Srinivasan, D. A. Case, and T. E. Cheatham, 2000. Calculating Structures and Free Energies of Complex Molecules: Combining Molecular Mechanics and Continuum Models. *Accounts of Chemical Research* 33:889–897.

14. Swanson, J. M. J., R. H. Henchman, and J. A. McCammon, 2004. Revisiting Free Energy Calculations: A Theoretical Connection to MM/PBSA and Direct Calculation of the Association Free Energy. *Biophysical journal* 86:67–74.

15. Brice, A. R., and B. N. Dominy, 2011. Analyzing the robustness of the MM/PBSA free energy calculation method: Application to DNA conformational transitions. *Journal of Computational Chemistry* 32:1431–1440.

16. Baker, N. A., D. Sept, S. Joseph, M. J. Holst, and J. A. McCammon, 2001. Electrostatics of nanosystems: Application to microtubules and the ribosome. *Proceedings of the National Academy of Sciences* 98:10037–10041.

17. Nina, M., D. Beglov, and B. Roux, 1997. Atomic Radii for Continuum Electrostatics Calculations Based on Molecular Dynamics Free Energy Simulations. *The Journal of Physical Chemistry B* 101:5239–5248.

18. Banavali, N. K., and B. Roux, 2002. Atomic Radii for Continuum Electrostatics Calculations on Nucleic Acids. *The Journal of Physical Chemistry B* 106:11026–11035.

19. Sitkoff, D., K. A. Sharp, and B. Honig, 1994. Accurate Calculation of Hydration Free Energies Using Macroscopic Solvent Models. *The Journal of Physical Chemistry* 98:1978–1988.

20. Karplus, M., and J. N. Kushick, 1981. Method for estimating the configurational entropy of macromolecules. *Macromolecules* 14:325–332.

21. Baron, R., W. F. van Gunsteren, and P. H. Hünenberger, 2006. Estimating the configurational entropy from molecular dynamics simulations: anharmonicity and correlation corrections to the quasi-harmonic approximation. *Trends Phys. Chem.* 11:87–122.

22. Baron, R., P. H. Hünenberger, and J. A. McCammon, 2009. Absolute Single-Molecule Entropies from Quasi-Harmonic Analysis of Microsecond Molecular Dynamics: Correction Terms and Convergence Properties. *Journal of Chemical Theory and Computation* 5:3150–3160.

23. Chang, C.-E., W. Chen, and M. K. Gilson, 2005. Evaluating the Accuracy of the Quasiharmonic Approximation. *Journal of Chemical Theory and Computation* 1:1017–1028.